

Article

Sensor for the characterization of 2D angular actuators with picoradian resolution and nanoradian accuracy on the microradian range

Marco Pisani ¹, Milena Astrua ¹ and Srijith Thirumalaj ²

¹ Istituto Nazionale di Ricerca Metrologica, INRIM;

² Politecnico di Torino;

* Correspondence: m.pisani@inrim.it; Tel.: +39 011 3919966

Abstract: High precision angular actuators are used for high demanding applications such as laser steering for photolithography. Piezo technology allows developing actuators with such a high resolution that the characterization of the same is out of the capabilities of commercially available instruments. At INRIM we have designed and built a device to the purpose of characterizing precision 2D angular actuators with a resolution surpassing the best devices on the market. The device is based on a multi reflection scheme that allows multiplying the deflection angle by a factor of 70. The ultimate resolution of the device is 2 prad/ $\sqrt{\text{Hz}}$ over a measurement range of 36 μrad with a measurement band > 10 kHz. The working principle, the practical realization and the case study on a top-level commercial angular actuator (Nano-MTA2 produced by MadCityLabs) are described.

Keywords: Angular actuators, angular sensors, encoders, autocollimators

1. Introduction

High precision angular positioning and measurements are crucial in a wide range of applications, such as beam steering mechanism and beam stabilization tasks in lithography, high precision stages and alignment of mechanical systems, measurement of the deflection angle of a cantilever in a scanning probe microscope or detection of gravitational waves. These are only few examples that highlight the need of high precision angular sensors and actuators.

Today on the market precision angular actuators able to tilt objects in one or two directions with exceptional precision are available. Most of these actuators are piezo driven and have integrated precision metrology such as strain gauges, optical encoders and capacitive sensors. Some examples of non-commercial devices can be found in ref [1-3]. The nominal resolution of these devices is as low as the nanoradian level, nevertheless the accuracy of the scale need to be calibrated and the real resolution must be verified. Finally, in some applications the time response must be characterized up to the kilohertz range.

In order to test such devices, high accuracy and traceable angle sensors are needed. The instruments with higher accuracy are autocollimators and interferometric systems. Autocollimators are optical instruments for precise measurements of small tilt angles of a reflecting mirror with a resolution of the order few nanoradians. They are commonly used for angle metrology [4, 5], but also for measuring straightness and parallelism of machine tools, flatness of surface plates and surface profilometry in synchrotron laboratories [6]. Traceability of autocollimators to the SI unit is obtained through a calibration against primary standards. Few National Metrology Institutes are able to calibrate autocollimators at the level of some tenths of microradian by means of top calibration facilities such as [7-12].

Angle sensors based on interferometric systems, such as Sagnac interferometers [13, 14], are directly traceable to the SI unit and can reach an extremely high sensitivity of the order of the picoradian over a limited angular range. The interferometer scheme based on a Mach-Zehnder

interferometer and described in [15] proved to reach a resolution of the order of $0.1 \text{ nrad}/\sqrt{\text{Hz}}$ over a wide angular range (i.e. $\pm 1.5 \text{ mrad}$), but it is not suitable for high frequencies.

The instrument described in this paper has been designed and built to the purpose of characterizing 2D angular actuators with a resolution better than $1 \text{ nrad}/\sqrt{\text{Hz}}$ in the band from 0.1 Hz to 10 kHz on two orthogonal axes. It is traceable to the SI unit through comparison with a calibrated autocollimator. The paper describes the working principle, the practical realization and the case study on a top-level commercial angular actuator.

2. Working principle

The measurement principle combines the effect of the optical lever (which converts a rotation of a mirror into a translation of a laser beam) and the reflection law (the rotation of the reflected beam is twice the rotation of the mirror), in a multiple reflection set-up. The principle of the angle amplification (AA) has been previously used as a high resolution autocollimator and described in [16]. A laser beam is sent towards a pair of quasi-parallel mirrors (see figure 1) and after N reflections exits from the same direction (solid line). Mirror A is glued to the tilting device to be measured while mirror B is kept fixed. When mirror A is rotated, the exiting mirror is rotated and translated proportionally to the distance between the two mirrors and N (dashed line). By using special mirrors and proper angles, N can be around 70 or more, leading to an enormous gain. A position sensitive detector measures the displacement of the output laser beam and converts it into an electric signal. The sensitivity of the device is better than $10^{-11} \text{ rad}/\sqrt{\text{Hz}}$.

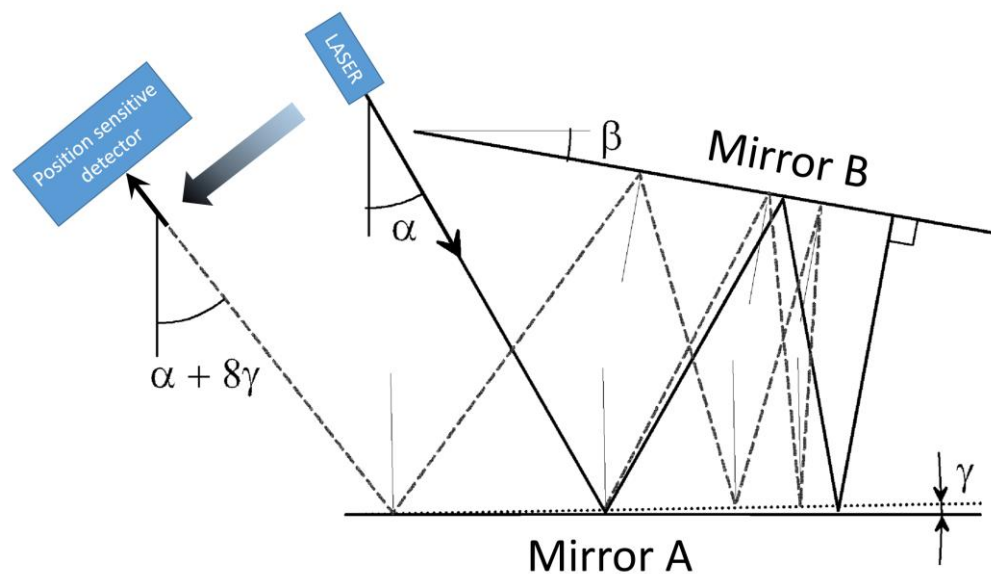


Figure 1. Ray tracing of the multiple reflection set-up showing the effect of the counter clockwise rotation of mirror A on the reflected beam. All angles in the figure are exaggerated for the sake of clarity. Incidence angle α is 30° , angle β between A and B is 10° , mirror B is rotated by $\gamma = 1^\circ$. In the initial condition, after three reflections ($\alpha / \beta = 3$) the laser beam impinges orthogonally on mirror B and is reflected back on its path. This auto collimation condition is close to the operative condition of the device. When mirror A is rotated by 1° counter clockwise, the beam is moved towards left and is rotated by 8 times γ .

3. Experimental set-up and case study

The picture of figure 2 depicts the experimental set-up. The key elements are highlighted in the picture. The laser beam is provided by a fiber coupled stabilized He-Ne laser (SIOS SL 02/1) ending on a fiber collimator mounted on a tilter. The laser is amplitude stabilized by its own electronics. The collimated beam, about 1 mm wide ($1/e$ at the lens) is sent to a folding mirror mounted on a high stability mirror mount. The combination of the collimator mount and the mirror mount allows to precisely aligning the beam to enter in the two mirrors assembly. The beam is reflected between the two high reflectivity mirrors and finally exits from the same side at a slightly lower height impinging on a second folding mirror that eventually sends the beam on a 2D position sensitive detector (PSD, UDT). A custom-made low noise electronics provides x and y output voltage and normalization with respect to the average power in order to reduce the effects of the residual amplitude noise of the laser. A polarizer is used to adjust the optical power on the PSD. The fixed “reference” mirror is mounted on a tip tilt optical mount driven by two motorized screws (Picomotor, New Focus, USA).

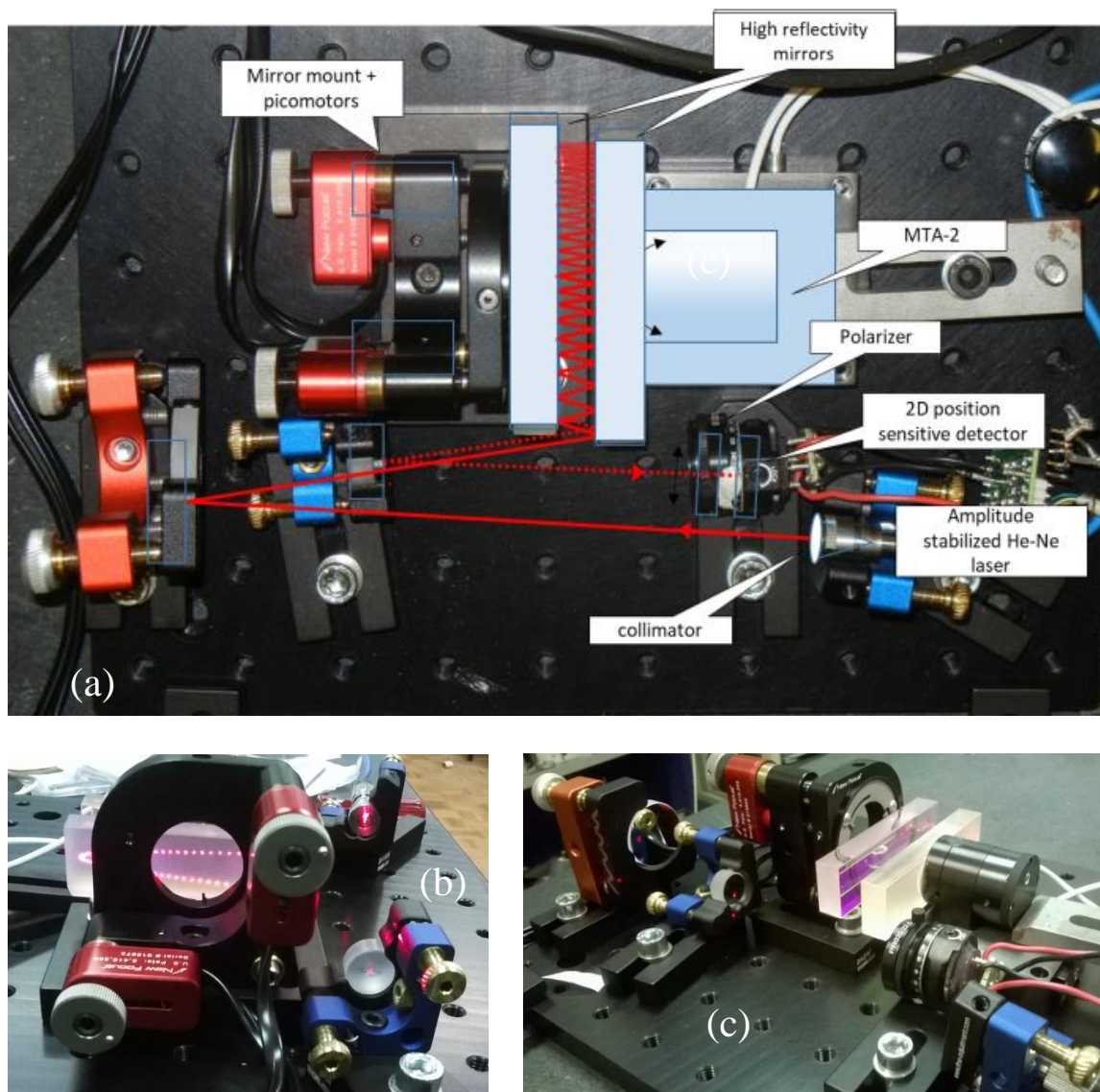


Figure 2. Pictures of the experimental set-up. (a): top view with the laser path drawn on the picture: the entering laser beam (solid red line) is sent towards the multiple reflection mirrors where the angle amplification occurs (see text for the details). (b): back view of the AA; the multi reflection pattern is visible at the back of the “reference” mirror. (c): side view of the AA; the DUT holding the “measurement” mirror is visible at top right.

The motorized screws are used to adjust the angle between the mirrors before the measurement set, and are switched off during the measurement. The moving “measurement” mirror is fixed to the device under test (DUT). Both the reference and the measurement mirrors are made of Clearceram®, have $\lambda/10$ flatness and are coated with a multilayer dielectric coating for a reflectivity better than 99.8 % at 633 nm. The two mirrors have a reflecting surface of 70 x 20 mm and are 10 mm thick. The distance between the mirrors is about 10 mm.

In the case presented here, we have tested the piezo-driven nano-actuator Nano-MTA2 produced by MadCityLabs (USA) [17] capable of 2 mrad p.p. full scale on two orthogonal axis. The MTA-2 is equipped with integrated piezoresistive “PicoQ” sensors with a nominal resolution of 4 nrad and a bandwidth of 400 Hz. The output of the piezoresistive sensor is used for the closed loop operation of the MTA; furthermore, is made available for the user in order to check the “real” angular displacement of the actuator. The MTA driver allows to drive the actuator with an external analog signal.

The experiment was realized in the INRIM’s “angle measurement” laboratory located underground in a thermally stabilized environment at $20\text{ }^{\circ}\text{C} \pm 0.1\text{ }^{\circ}\text{C}$.

4. Results and discussion

We have performed two kinds of measurements: the first is to characterize the noise of the AA and of the DUT in the frequency domain; the second is to characterize the resolution of the DUT in the time domain. All the measurements have been done for both vertical and horizontal axes of the DUT. In the following, only the results of the horizontal axis are shown, although the orthogonal axis has almost identical performances.

The whole experiment was mounted on a stable granite table (passively isolated) and enclosed in a wooden box to isolate for acoustic noises and air turbulences. The signals coming from the PSD are amplified and sent to a 16 bit 100 kS/s A/D converter and processed by a LabView® based software to calculate the noise spectral density. In figure 3 are summarized the results of the noise tests. The green curve represent the noise limit due to the laser noise, the detector noise and the electronics noise. It has been obtained sending the laser beam on the detector after only one reflection in order to include all noise sources besides mechanical ones. The blue curve is the noise spectral density of the sensor of the AA when the DUT is switched off. The noise is limited by the environmental disturbances (mainly mechanical vibrations) coupled to the mechanical structure. The dashed red line indicates the 1 nrad/ $\sqrt{\text{Hz}}$ level for reference. The performances could be further ameliorated by a better acoustic and vibration isolation, although the environment was very quiet. Finally, the DUT is switched on and the noise curve is plotted in red. The difference between the blue and the red curves shows that we are measuring the “real” noise performance of the actuator when in working mode, that in this case is basically due to the noise of the active control system. Finally, at frequencies above 3 kHz the angular noise of the device reaches the electronics noise floor of the AA.

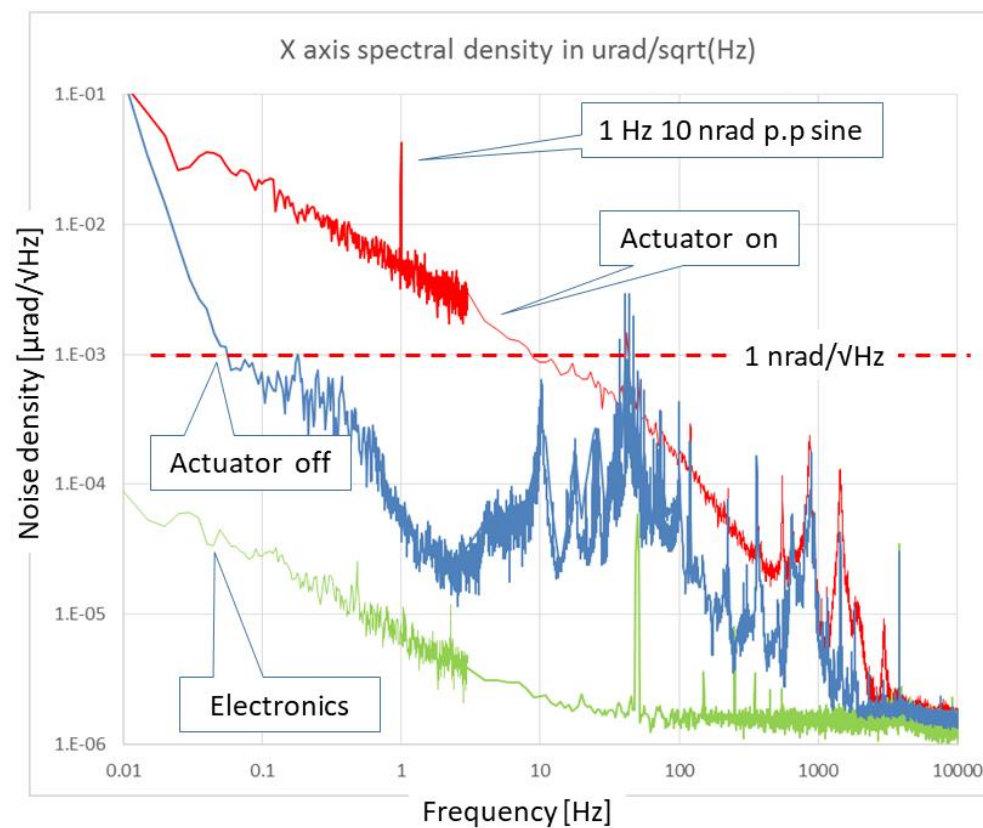


Figure 3. Noise spectral density curves of the output signal of the measuring device in three different conditions. The meaning of the three curves is explained in the text. Y axis analysis is not shown, but the behavior is very similar to X axis.

In figure 4 are summarized the results of the time domain resolution tests. A small signal is sent to the MTA-2 to drive the actuator with a square angular signal having nominal amplitude of 25 nrad p.p. at 1 Hz . The blue and red curves are the output of the calibration device low pass filtered respectively at 10 kHz and 1 kHz showing the “real” behaviour of the DUT. The green, purple and turquoise curves are the output of the Nano-MTA2 sensor low pass filtered respectively at 30 Hz , 1 kHz and 10 kHz . It is evident that the output of the integrated piezoresistive sensor of the actuator underestimates the real noise of the same at low frequencies (green curve), since is a measurement taken “in the control loop”. On the other hand, at high frequencies, the noise of the sensor is higher than the real noise of the actuator (purple and turquoise curves) which are hence overestimated. In any case, the exceptionally good resolution of the actuator under test is demonstrated with this experiment.

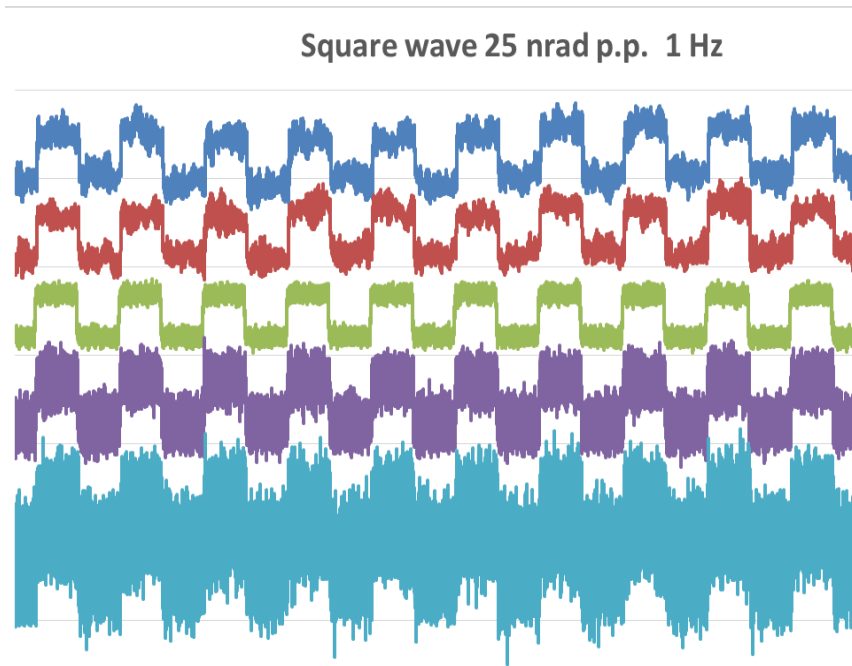


Figure 4. Time domain characterization of the MTA-2. The meaning of the various tracks is explained in the text. The vertical scale is the same for all tracks.

In figure 5 is shown the noise of the MTA PicoQ sensor recorded when the system is at rest. This noise has the effect to limit the effective resolution of the device and, as shown in figure 4, to overestimate the “real” angular noise of the MTA for frequencies higher than 10 Hz and to underestimate the noise for frequencies lower than 10 Hz. Considering that the full scale of the sensor is 2 mrad full scale it is evident the exceptional dynamic range of the sensor exceeding 7 orders of magnitude.

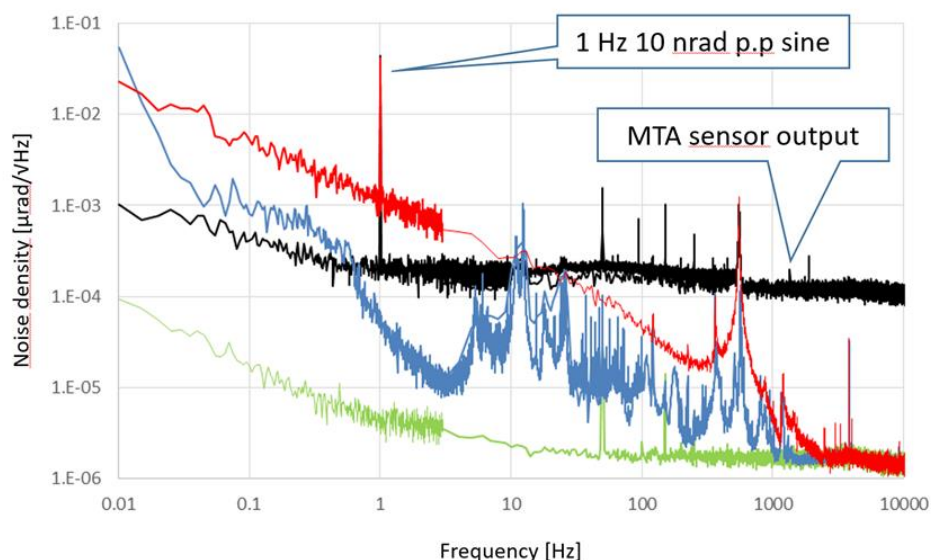


Figure 5. Noise of the MTA sensor: the black curve added to the noise spectral density analysis shows the noise of the MTA PicoQ sensor, which has the effect to limit the effective resolution of the device and, as shown in figure 4, to overestimate the “real” angular noise of the MTA at high frequencies.

The resolution of the angle amplifier (AA) in the present setup is limited by acousto-mechanic disturbances coupling with the mechanical resonances of the actuator mainly present in the range between a few Hz up to 1 kHz. A wooden cover was used to reduce acoustic noise at high frequencies. In figure 6 is shown the spectrum of the noise measured in proximity of the AA with and without the wooden cover. It is easy to find the peak at 10 Hz and the noise between 10 to 1000 Hz in the blue spectrum of fig 3. The ultimate limit of the AA is the white noise of the electronics, which has a floor at 2 $\mu\text{rad}/\sqrt{\text{Hz}}$.

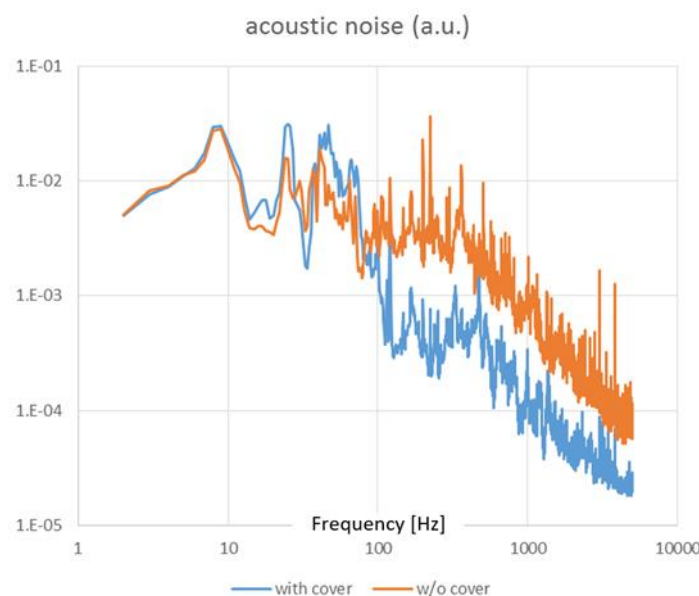


Figure 6. Acoustic noise measured in proximity of the AA with and without the wooden cover expressed in arbitrary units. It is evident that dominant frequencies in the 10-100 Hz range are not shielded by the cover and could be eliminated by further damping and isolation.

5. Calibration of the AA

In order to convert the voltage generated by the PSD electronics into an angle, a calibration is needed. Although in principle it is possible to model the shift of the beam caused by the rotation of the mirror by means of basic ray tracing analysis, it is much easier and reliable to make use of a direct comparison with a reference standard. Therefore, we have performed a calibration of the DUT on the full scale to check for the scale factor and linearity of the same. The calibration has been undertaken by direct comparison with a reference autocollimator (ELCOMAT HR by Moeller-Wedel, Germany), in turn calibrated against the INRIM angle standard [12].

The autocollimator (AC) is placed at the back side of the AA aiming at an auxiliary mirror glued on top of the mirror fixed to the MTA. The MTA is driven in steps of known nominal value and the output of the AC is recorded together with the output of the AA electronics. The slope in the interval is calculated for both axis (being about 1.8 $\mu\text{rad}/\text{V}$) and is used to convert the output of the ADC board directly into radian units. The uncertainty of the conversion factor has been calculated taking in account the uncertainty and the resolution of the AC and the non-linearity of the PSD sensor in the area of interest. An uncertainty less than 0.1 % is assigned to the scale factor. The full scale range in the presented configuration is 36 $\mu\text{rad} \approx 7.4$ arcsec. For angular intervals of the order of microradian this uncertainty is dominant, when working at the nanoradian scale the error sources coming from the noise are dominant and the time interval of the measurement must be taken into account.

6. Conclusions

We have realized a simple and effective set-up used to calibrate and characterize precision piezoelectric nano-angle actuators on two orthogonal axes. The noise of the device (here called AA) is limited by environmental disturbances to less than 1 nrad/ $\sqrt{\text{Hz}}$ for frequencies higher than 0.1 Hz and is as low as 2 prad/ $\sqrt{\text{Hz}}$ for frequencies higher than 3 kHz. The frequency range is > 10 kHz. These performances are better than any measurement device and angular actuator available on the market to the knowledge of the authors. The traceability is guaranteed through the use of a reference autocollimator calibrated against the INRIM angular standard. With a practical experiment we have demonstrated the feasibility of the calibration and dynamic characterization of a top level commercial device. The method allowed to find the real performances of the DUT demonstrating that relying on the internal sensor the noise can be underestimated or overestimated depending on the frequency band.

Author Contributions: Conceptualization, Marco Pisani and Milena Astrua; realization of the experiment, Marco Pisani and Srijiith Thirumalaj; data collection and analysis, all authors. All authors have read and agreed to the published version of the manuscript.

Funding: This research received no external funding.

Acknowledgments: The authors wish to acknowledge their colleague Massimo Zucco who wrote the software for the spectral density analysis and Emanuele Audrito for his technical support in realizing the hardware.

Conflicts of Interest: The authors declare no conflict of interest. Authors do not have any professional relationship with the firm Mad City Labs. The funds and human resources used for the study are from institutional funds for research in the field of angular metrology.

References

1. S. G. Alcock et al. A novel instrument for generating angular increments of 1 nanoradian Rev. Sci. Instrum. 86, 125108 (2015)
2. D. Shu et al. Development and application of a two-dimensional tip-tilting stage system with nanoradian-level positioning resolution Nuclear Instruments and Methods in Physics Research A 649 (2011) 114–117
3. X. Tan et al. Two-Dimensional Micro-/Nanoradian Angle Generator with High Resolution and Repeatability Based on Piezo-Driven Double-Axis Flexure Hinge and Three Capacitive Sensors Sensors 2017, 17, 2672
4. Kim J-A et al. Calibration of angle artifacts and instruments using a high precision angle generator Int. J. Precis. Eng. Manuf. 14, 367–371 (2013)
5. Stone J A, Amer M, Faust B and Zimmermann J 2004 Uncertainties in small-angle measurement systems used to calibrate angle artifacts J. Res. Natl Inst. Stand. Technol. 109 2004
6. Siewert F et al. 2012 Ultra-precise characterization of LCLS hard x-ray focusing mirrors by high resolution slope measuring deflectometry Opt. Express 20 4525–36
7. Probst R et al., 1998 The new PTB angle comparator Meas. Sci. Technol. 9 1059–66
8. Yandayan T et al. High precision small angle generator for realization of the SI unit of plane angle and calibration of high precision autocollimators 2012 Meas. Sci. Technol. 23 094006
9. B J Eves The NRC autocollimator calibration facility Metrologia 50 (2013) 433–440
10. V Heikkinen et al. Interferometric 2D small angle generator for autocollimator calibration Metrologia 54 (2017) 253–261
11. Watanabe T, Fujimoto H and Masuda T Self-Calibratable Rotary Encoder 2005 J. Phys.: Conf. Ser. 13 240–45
12. Pisani M and Astrua M The new INRIM rotating encoder angle comparator (REAC) 2017 Meas. Sci. Technol. 28 (2017) 045008

13. J M Hogan et al. Precision angle sensor using an optical lever inside a Sagnac interferometer OPTICS LETTERS Vol 36 No 9 May 1 2011
14. P. B. Dixon et al. Ultrasensitive Beam Deflection Measurement via Interferometric Weak Value Amplification Physical Review Letters 102, 173601 (2009)
15. J.G. Park and K. Cho, High-precision tilt sensor using a folded Mach-Zehnder geometry in-phase and quadrature interferometer, Appl. Opt 55 (2016)
16. Pisani M, Astrua M, "Angle amplification for nanoradian measurements," Appl. Opt. 45 (2006) 1725-1729
17. <http://www.madcitylabs.com/nanomtaseres.html>